# Interactions of Phenyldithioesters with Gold Nanoparticles (AuNPs): Implications for AuNP Functionalization and Molecular Barcoding of AuNP Assemblies

**ARTICLE** *in* LANGMUIR · OCTOBER 2009

Impact Factor: 4.46 · DOI: 10.1021/la9023162 · Source: PubMed



**4 AUTHORS**, INCLUDING:

Idriss Blakey
University of Queensland
**98** PUBLICATIONS **882** CITATIONS
SEE PROFILE

Tara Schiller
The University of Warwick
**38** PUBLICATIONS **579** CITATIONS
SEE PROFILE

Zulkifli Merican
**23** PUBLICATIONS **126** CITATIONS
SEE PROFILE

Langmuir Article

pubs.acs.org/Langmuir


# Interactions of Phenyldithioesters with Gold Nanoparticles (AuNPs): Implications for AuNP Functionalization and Molecular Barcoding of AuNP Assemblies

Idriss Blakey,*[,†] Tara L. Schiller,[‡] Zul Merican,[†] and Peter M. Fredericks[‡]

[†]*The University of Queensland, Australian Institute for Bioengineering and Nanotechnology and Centre for Magnetic Resonance, Queensland, Australia, 4072, and* [‡]*Queensland University of Technology, School of Physical and Chemical Sciences, Queensland, Australia, 4001*

*Received June 28, 2009. Revised Manuscript Received August 28, 2009*

The interactions of phenyldithioesters with gold nanoparticles (AuNPs) have been studied by monitoring changes in the surface plasmon resonance (SPR), depolarised light scattering, and surface enhanced Raman spectroscopy (SERS). Changes in the SPR indicated that an AuNP-phenyldithioester charge transfer complex forms in equilibrium with free AuNPs and phenyldithioester. Analysis of the Langmuir binding isotherms indicated that the equilibrium adsorption constant, $K_{ads}$, was $2.3 \pm 0.1 \times 10^6$ $M^{-1}$, which corresponded to a free energy of adsorption of $36 \pm 1$ kJ $mol^{-1}$. These values are comparable to those reported for interactions of aryl thiols with gold and are of a similar order of magnitude to moderate hydrogen bonding interactions. This has significant implications in the application of phenyldithioesters for the functionalization of AuNPs. The SERS results indicated that the phenyldithioesters interact with AuNPs through the C═S bond, and the molecules do not disassociate upon adsorption to the AuNPs. The SERS spectra are dominated by the portions of the molecule that dominate the charge transfer complex with the AuNPs. The significance of this in relation to the use of phenyldithioesters for molecular barcoding of nanoparticle assemblies is discussed.

## Introduction

Functionalized gold nanoparticles (AuNPs) have been touted to be useful in a range of applications including, biomolecule detection,[1−5] imaging enhancement probes,[6] drug delivery,[7] nanolithography,[8] phototherapy,[9,10] and catalysis.[11] Functionalization of AuNPs with small molecules or polymers is a crucial step in developing materials for these applications. A range of molecules are known to interact with gold surfaces. These include thiols, disulfides, isothiocyanates, isocyanides, dithiocarbamates, dithioesters, and trithiocarbonates. By far the most extensively studied groups are thiols and the closely related disulfides. Some of the most important observations in this field are that thiols and disulfides are known to dissociate upon binding to flat gold surfaces and gold nanoparticles. Although a covalent bond is believed to form between the sulfur and gold, the bond is relatively weak in that the bound ligands are in equilibrium with free thiols in solution.[12] This second observation in particular is important for functionalization of AuNPs by ligand exchange.[12] However, it must be kept in mind that the effectiveness of ligand exchange reactions can be dependent on the exact structure of the thiol. Recently, dithiocarbamates have been investigated as a versatile strategy for the functionalization of and controlled assembly of AuNPs.[13−19] However, the interactions of the other compounds mentioned above with AuNPs have not been characterized to the same degree. In particular, the interactions of dithioesters, dithiocarbonates and trithiocarbonates functional groups with gold have only limited literature reports.[20−22] These classes of compounds, as well as substituted dithiocarbamates, have received significant attention over the past ten years, due to the interest in them as agents for controlling reversible addition−fragmentation chain transfer (RAFT) polymerization, where these compounds can result in polymers with controlled molecular weights, low

*Corresponding author. E-mail: i.blakey@uq.edu.au.

(1) Cao, Y. C.; Jin, R.; Mirkin, C. A. *Science* (*Washington, D.C.*) **2002**, *297*, 1536–1540.
(2) Di, J.; Shen, C.; Peng, S.; Tu, Y.; Li, S. *Anal. Chim. Acta* **2005**, *553*, 196–200.
(3) Grubisha, D. S.; Lipert, R. J.; Park, H.-Y.; Driskell, J.; Porter, M. D. *Anal. Chem.* **2003**, *75*, 5936–5943.
(4) Kneipp, K.; Haka, A. S.; Kneipp, H.; Badizadegan, K.; Yoshizawa, N.; Boone, C.; Shafer-Peltier, K. E.; Motz, J. T.; Dasari, R. R.; Feld, M. S. *Appl. Spectrosc.* **2002**, *56*, 150–154.
(5) Wang, Z.; Lee, J.; Cossins, A. R.; Brust, M. *Anal. Chem.* **2005**, *77*, 5770–5774.
(6) Kneipp, J.; Kneipp, H.; McLaughlin, M.; Brown, D.; Kneipp, K. *Nano Lett.* **2006**, *6*, 2225–2231.
(7) Radt, B.; Smith, T. A.; Caruso, F. *Adv. Mater.* (*Weinheim, Ger.*) **2004**, *16*, 2184–2189.
(8) Cortie, M. B.; Harris, N.; Ford, M. J. *Physica B* (*Amsterdam, Neth.*) **2007**, *394*, 188–192.
(9) Huang, X.; Jain, P. K.; El-Sayed, I. H.; El-Sayed, M. A. *Photochem. Photobiol.* **2006**, *82*, 412–417.
(10) Pissuwan, D.; Valenzuela, S. M.; Miller, C. M.; Cortie, M. B. *Nano Lett.* **2007**, *7*, 3808–3812.
(11) Zhang, Z.-F.; Cui, H.; Lai, C.-Z.; Liu, L.-J. *Anal. Chem.* **2005**, *77*, 3324–3329.
(12) Caragheorgheopol, A.; Chechik, V. *Phys. Chem. Chem. Phys.* **2008**, *10*, 5029–5041.
(13) Sanchez-Cortes, S.; Domingo, C.; Garcia-Ramos, J. V.; Aznarez, J. A. *Langmuir* **2001**, *17*, 1157–1162.
(14) Wessels, J. M.; Nothofer, H.-G.; Ford, W. E.; von Wrochem, F.; Scholz, F.; Vossmeyer, T.; Schroedter, A.; Weller, H.; Yasuda, A. *J. Am. Chem. Soc.* **2004**, *126*, 3349–3356.
(15) Zhao, Y.; Perez-Segarra, W.; Shi, Q.; Wei, A. *J. Am. Chem. Soc.* **2005**, *127*, 7328–7329.
(16) Morf, P.; Raimondi, F.; Nothofer, H.-G.; Schnyder, B.; Yasuda, A.; Wessels, J. M.; Jung, T. A. *Langmuir* **2006**, *22*, 658–663.
(17) Vickers, M. S.; Cookson, J.; Beer, P. D.; Bishop, P. T.; Thiebaut, B. *J. Mater. Chem.* **2006**, *16*, 209–215.
(18) Park, M.-H.; Ofir, Y.; Samanta, B.; Rotello, V. M. *Adv. Mater.* (*Weinheim, Ger.*) **2009**, *21*, 2323–2327.
(19) Park, M.-H.; Ofir, Y.; Samanta, B.; Arumugam, P.; Miranda, O. R.; Rotello, V. M. *Adv. Mater.* (*Weinheim, Ger.*) **2008**, *20*, 4185–4188.
(20) Merican, Z.; Schiller, T. L.; Hawker, C. J.; Fredericks, P. M.; Blakey, I. *Langmuir* **2007**, *23*, 10539–10545.
(21) Duwez, A.-S.; Guillet, P.; Colard, C.; Gohy, J.-F.; Fustin, C.-A. *Macromolecules* **2006**, *39*, 2729–2731.
(22) Hotchkiss, J. W.; Lowe, A. B.; Boyes, S. G. *Chem. Mater.* **2007**, *19*, 6–13.

polydispersities and controlled end groups.[23−26] As a result of this, a diverse range of compounds have been synthesized from these classes of functional groups in the past 10 years. These classes of compounds are compatible with a range of functional groups, and as such thiocarbonylthio compounds with a range of reactive functional groups have been synthesized. Some of these include carboxylic acids,[27] alcohols, phosphonates,[27] acetylenes,[28] epoxy,[29] azides,[30] pentafluorophenyl esters,[31] and pyridyldisulfides.[32] Furthermore, RAFT agents containing H-bonding groups[33] pyrene,[34] azobenzene,[35] proteins,[36] ionic liquids,[37] cholesterol,[38] and lipids[39] have also been synthesized. Although the original intent was to use these compounds for controlled polymer synthesis, this wide array of compounds could potentially be useful for the synthesis of functionalized gold nanoparticles. However, for this to occur a more detailed understanding of the interactions of thiocarbonylthio compounds with AuNPs is required.

Duwez et al.[21] demonstrated that small molecule dithioesters and trithiocarbonates bind to flat gold surfaces. They assessed the specific binding modes using X-ray photoelectron spectroscopy (XPS) where they concluded that binding was bidentate, i.e., via both sulfur groups in the dithioester. There have also been reports of dithiocarbamates binding to gold surfaces where the specific mode of binding was assessed using surface enhanced Raman spectroscopy (SERS). These studies concluded that the mode of binding could be either monodentate or bidentate and the particular binding mode was dependent on the density of ligands.[13,40] Similar studies have also been reported for bis- and tris(thiol) compounds.[41] To our knowledge there have been no studies investigating the adsorption equilibrium coefficients of thiocarbonylthio compounds in general. In this contribution we investigate the formation of charge transfer complexes of phenyldithioesters with AuNPs and determine equilibrium coefficients of adsorption using UV−visible spectroscopy and depolarized light scattering. Using SERS, we also further demonstrate the mode of binding of these compounds to the AuNP surface and further explore the electronic interactions of phenyldithioesters with AuNPs and how this effects the SERS observed from the molecule-AuNP complexes.

## Experimental Section

**Materials.** *S*-(Thiobenzoyl)thioglycolic acid (**PDE-1**), 1 M phenylmagnesium bromide solution in THF, carbon disulfide, α-bromophenylacetate, $HAuCl_4$, sodium citrate, AIBN, triethyl amine, thionyl chloride, 3-butynol, bromophenylacetic acid, and butynyl bromophenylacetate were obtained from Sigma Aldrich or a subsidiary. Tetrahydrofuran, diethyl ether, ethyl acetate, dichloromethane, and hexane were obtained from Merck.

**Synthesis of Ethyl 2-Phenyl-2-(phenylcarbonothioylthio)-acetate (PDE-2).** Phenyl magnesium bromide (25 mL, 25 mmol) in tetrahydrofuran was cooled to 0 °C in an ice−water bath. Carbon disulfide (1.904 g, 25 mmol) was then added dropwise to give a red solution. After the solution was stirred for 60 min, α-bromophenylacetate (6.08 g, 25 mmol) was added dropwise. The solution was allowed to warm to room temperature and react and was stirred for 16 h. The reaction mixture was filtered and the tetrahydrofuran was removed under reduced pressure. The mixture was dissolved in diethyl ether, which was then extracted with water, 0.5 M $NaHCO_3$, 1% HCl, and water using three washes of each. The organic layer was concentrated using rotary evaporation at reduced pressure. The crude product was purified by column chromatography using silica gel as the stationary phase, with 5% ethyl acetate and 95% hexane as the mobile phase. Purity of the fractions was initially tested by FTIR-ATR of the dried fraction. A dark red crystalline solid was obtained with an 81% purified yield. $^1$H NMR 400 MHz (CDCl3): $\delta$ (ppm)) 8.01−7.99 (m, 2H, Ar**H**), 7.51−7.48 (m. 3H, Ar**H**), 7.37−7.33 (m, 5H, Ar**H**), 5.73 (s, 1H, Ph**H**), 4.28−4.19 (m, 2H, $-OC\mathbf{H_2}CH_3$), 1.28−1.24 (t, 3H, $-OCH_2C\mathbf{H_3}$). $^{13}$C NMR 400 MHz, (CDCl3): $\delta$ (ppm)) 225.81 (**C**=S), 168.71 (**C**=O), 143.86, 133.37, 132.66, 128.93, 128.74, 128.72, 128.29, 126.84, 62.15 (**SC**Ph), 58.82 ($-\mathbf{OC}H_2CH_3$), 13.97 ($-OCH_2\mathbf{C}H_3$). *m*/*z* MS/MS (APCI$^+$): $[C_{17}H_{17}O_2S_2]^+$ [M + H] 317.08 (calcd 317.07)

**Synthesis of But-3-ynyl 2-Bromo-2-phenylacetate.** α-bromophenylacetic acid (13.95 mmol) was dissolved in $SOCl_2$ ($2.74 \times 10^{-1}$ mol) and was refluxed under an atmosphere of nitrogen for 2 h. After which the excess $SOCl_2$ was removed by vacuum distillation at room temperature. The resulting acyl chloride was obtained as a light brownish yellow oil which was added dropwise to an anhydrous solution of 3-butyn-1-ol (69.76 mmol) and $Et_3N$ (3.1 g) in DCM (13.9 mL) under an atmosphere of argon. The mixture was allowed to react with stirring overnight. At the end of the reaction the reaction mixture was filtered and the filtrate was washed with dilute (0.1 M) HCl (1×), water and sodium bicarbonate (1×), and water in series. The organic fraction was dried over $MgSO_4$. Solvent was removed by rotary evaporation to give a light yellow oil, sufficiently pure to be used in a subsequent reaction. Yield: 1.78 g. (48% yield) $^1$HNMR (300 MHz, $CHCl_3$-$d_3$): $\delta$ (ppm) 1.93 (t, 1H, **CH** terminal acetylene), 2.46 (m, 2H, $-CH_2-\mathbf{CH_2}CCH$), 4.20 (2H, m, $-\mathbf{CH_2}CH_2CCH$), 5.36 (s, 1H, Br−**CH**−ArCO), 7.32−7.34 (m, 3H, Ar**H**), 7.46 (m, 2H, Ar**H**).

**Synthesis of 3-ynyl 2-Phenyl-2-(phenylcarbonothioylthio)-acetate (PDE-3).** A 1 M phenylmagnesium bromide solution (5.38 mmol) was warmed to 40 °C and $CS_2$ (5.38 mmol) was added dropwise, resulting in a clear red color solution. The solution was cooled to 25 °C and stirred for another 15 min after which but-3-ynyl 2-bromo-2-phenylacetate (5.93 mmol) was added. The reaction mixture was heated to 80 °C and was stirred for 24 h. The reaction was worked up by adding ice-cold water, and the aqueous layer was extracted with diethyl ether (3x). The combined organic layers were rinsed with $H_2O$ and dried over $MgSO_4$. Excess solvent was removed by rotary evaporation, and the crude product was purified by column chromatography with silica as a stationary phase (2−7% ethyl acetate/hexane). Yield: 1.2 g of a dark red liquid. $^1$H NMR (300 MHz, $CDCl_3$): $\delta$ 1.95 (t, 1H, **CH** terminal acetylene), 2.53 (t, 2H, $-CH_2\mathbf{CH_2}CCH$), 4.19 (2H,

(23) Barner-Kowollik, C.; Davis, T. P.; Heuts, J. P. A.; Stenzel, M. H.; Vana, P.; Whittaker, M. *J. Polym. Sci., Part A: Polym. Chem.* **2003**, *41*, 365–375.
(24) Moad, G.; Chong, Y. K.; Postma, A.; Rizzardo, E.; Thang, S. H. *Polymer* **2005**, *46*, 8458–8468.
(25) Perrier, S.; Takolpuckdee, P.; Westwood, J.; Lewis, D. M. *Macromolecules* **2004**, *37*, 2709–2717.
(26) Plummer, R.; Hill, D. J. T.; Whittaker, A. K. *Macromolecules* **2006**, *39*, 8379–8388.
(27) Boyer, C.; Bulmus, V.; Priyanto, P.; Teoh, W. Y.; Amal, R.; Davis, T. P. *J. Mater. Chem.* **2009**, *19*, 111–123.
(28) Ranjan, R.; Brittain, W. J. *Macromol. Rapid Commun.* **2007**, *28*, 2084–2089.
(29) Vora, A.; Nasrullah, M. J.; Webster, D. C. *Macromolecules* **2007**, *40*, 8586–8592.
(30) Chen, F.; Cheng, Z.; Zhu, J.; Zhang, W.; Zhu, X. *Eur. Polym. J.* **2008**, *44*, 1789–1795.
(31) Roth, P. J.; Wiss, K. T.; Zentel, R.; Theato, P. *Macromolecules* **2008**, *41*, 8513–8519.
(32) Liu, J.; Liu, H.; Boyer, C.; Bulmus, V.; Davis, T. P. *J. Polym. Sci., Part A: Polym. Chem.* **2009**, *47*, 899–912.
(33) Bernard, J.; Lortie, F.; Fenet, B. *Macromol. Rapid Commun.* **2009**, *30*, 83–88.
(34) Meuer, S.; Braun, L.; Schilling, T.; Zentel, R. *Polymer* **2009**, *50*, 154–160.
(35) Wan, X.; Zhu, X.; Zhu, J.; Zhang, Z.; Cheng, Z. *J. Polym. Sci., Part A: Polym. Chem.* **2007**, *45*, 2886–2896.
(36) De, P.; Li, M.; Gondi, S. R.; Sumerlin, B. S. *J. Am. Chem. Soc.* **2008**, *130*, 11288–11289.
(37) Coady, D. J.; Norris, B. C.; Lynch, V. M.; Bielawski, C. W. *Macromolecules* **2008**, *41*, 3775–3778.
(38) Segui, F.; Qiu, X.-P.; Winnik, F. M. *J. Polym. Sci., Part A: Polym. Chem.* **2008**, *46*, 314–326.
(39) Bathfield, M.; Daviot, D.; D'Agosto, F.; Spitz, R.; Ladaviere, C.; Charreyre, M.-T.; Delair, T. *Macromolecules* **2008**, *41*, 8346–8353.
(40) Sanchez-Cortes, S.; Garcia-Ramos, J. V. *Surf. Sci.* **2001**, *473*, 133–142.
(41) Park, J.-S.; Vo, A. N.; Barriet, D.; Shon, Y.-S.; Lee, T. R. *Langmuir* **2005**, *21*, 2902–2911.

m, $-CH_2CH_2CCH$), 5.73 (s, 1H, -CH-ArCO), 7.37−7.52 (m, 8H, ArH), 7.99 (m, 2H, ArH). $^{13}C$ NMR (400 MHz, $CDCl_3$): $\delta$ 18.8, 58.7, 63.63, 70.11, 126.93, 128.40, 128.87, 129.04, 130.23, 130.47, 132.80, 133.02, 143.87, 168.58, 225.92. Anal. Calcd C, 67.03; H, 4.74; S, 18.84. Found: C, 66.98; H, 4.48; S, 18.60. *m/z* (ES−MS) $[C_{18}H_{24}NO_3^+]$: 302.02 (calcd 302.18).

**Gold Nanoparticle Synthesis.** All glassware was cleaned in aqua regia, rinsed in ultrapure water, then oven-dried. AuNPs were synthesized using the citrate reduction method according to Frens[42] and Sutherland.[43] 100 mL of 1 mM $HAuCl_4$ was brought to the boil then 3.5 mL of 17.5 mM sodium citrate was added. The solution was refluxed for a further 15 min to ensure complete reduction. The AuNPs were characterized by UV−vis spectroscopy $A_{SPRmax}$ 0.6688 (2× dilution), $\lambda_{SPRmax}$ 520 nm, which corresponds to a mean diameter of 15 nm,[44] Dynamic light scattering (DLS) median diameter 16 ± 2 nm and TEM 16 ± 1 nm. On the basis of the size from TEM and the amount of gold added during synthesis, the concentration of AuNPs was calculated to be 2.1 nM. In many of the experiments the solutions were diluted by a factor of 2.

**Measurement of Charge Transfer Complex Formation.** A solution of as synthesized gold nanoparticles (1.5 mL) was added to a 1 cm quartz cuvette, which was then diluted with Milli-Q water (1.5 mL), which resulted in a solution that had an absorbance less than 1 at the surface plasmon resonance maxima. Sequential addition of solutions of PDE-1 (0.01 mg/mL, 47 $\mu$M)) to the cuvette were made, where a typical addition was 2 $\mu$L. After an addition the cuvette was stopperred and inverted several times to allow thorough mixing. The solution was left to stand for at least 2 min prior to measurement via UV−vis spectrometry.

**Depolarized Light Scattering.** Depolarized light scattering spectra were collected using a Horiba Jobin-Yvon Fluoromax 4 spectrofluorometer, which has monochromators for the excitation and emission and is fitted with automated polarizers at excitation and emission such that scattering spectra could be collected in VV, VH, HV, and HH positions. The angle of collection was 90° to the excitation source. The spectrofluorometer polarizers were calibrated for anisotropy experiments according to the manufacturers instructions prior to use, and the *G* value of the instrument was also determined using a Ludox solution (where $G = I_{HV}/I_{HH}$). For samples collected in a 1 cm path-length cell the nanoparticle solutions were typically diluted to a concentration of approximately 50 pm of nanoparticles.

**Collection of Surface-Enhanced Raman and Raman spectra.** Raman and SERS spectra were collected on a ThermoFischer Almega dispersive Raman spectrometer. Thin films were measured using the microscope accessory with a 10× or 50× aperture and liquids/solutions were typically measured using the 180° backscatter accessory. The instrument is fitted with both 633 and 785 nm lasers. For the wavelength used, refer to the text in Results and Discussion. Unless otherwise stated the spectra were collected using a single grating between 90- 3900 $cm^{-1}$, in low resolution mode with at least 32 scans.

FT Raman and FT-SERS spectra were collected on a ThermoFischer DXR FT Raman module, operating in 180° backscatter mode. The NIR laser wavelength was 1064 nm and typically the laser power was set to 0.5W which corresponded to approximately 0.32 W at the sample

## Results and Discussion

**Interactions of PDE-1 with AuNPs.** The strong absorbance of AuNPs in the visible region are widely known to be a result of surface plasmon resonances (SPR) (see Figure 1), which occur due to collective oscillations of conduction electrons on the surface of

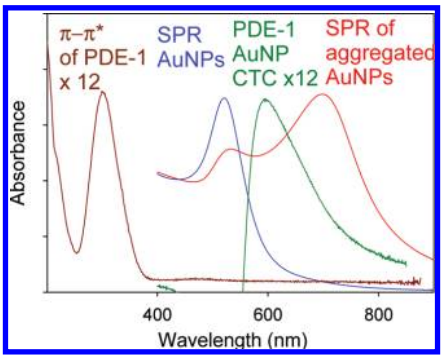


**Figure 1.** From left to right UV−vis spectrum shows; the absorption spectrum of 5 $\mu$M PDE-1 (purple, intensity x 12), which has a prominent $\pi-\pi$ * transition at 300 nm; the SPR of 1.05 nM of unaggregated AuNPs (blue); the AuNP···PDE-1 charge transfer complex resonance (green) which was obtained by subtraction of a spectrum of unmodified AuNPs; the SPR of 2 nM aggregated AuNPs (red) where spectrum was collected for AuNPs undergoing aggregation for 20 min following addition of PDE-2 (total concentration 24 $\mu$M).

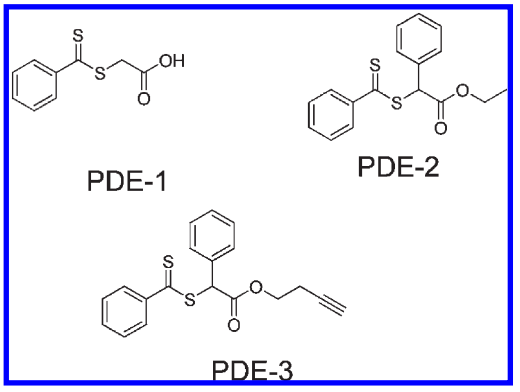


**Figure 2.** Structures of phenyldithioester derivatives used in this study.

NPs that are induced by an external electromagnetic field.[45] The SPR of AuNPs is sensitive toward a number of factors, such as nanoparticle size and shape, refractive index of surrounding environment, formation of charge transfer complexes with small molecules and degree of aggregation. Aggregation of nanoparticles can cause large shifts in the SPR, due to formation of quadrupole interactions,[46] which dominate any changes in SPR from formation of charge transfer complexes and changes in refractive index. Above the critical aggregation concentration, hydrophobic phenyldithioesters such as PDE-2 and PDE-3 (see Figure 2) cause the AuNP surface to be hydrophobic, which is the driving force for aggregation (see Figure 1). However, stabilization of AuNPs with negatively charged small molecule has been reported to avoid aggregation. For example, Wiederrecht et al.[47,48] were able to stabilize gold and silver nanoparticles with a negatively charged thiacyanine dye which prevented aggregation. This allowed study of the interaction of dye molecules with nanoparticles and the effect of this interaction on the resultant optical properties without interference from aggregation.

(42) Frens, G. *Nature* (*London, U. K.*) **1973**, *241*, 20–22.
(43) Sutherland, W. S.; Winefordner, J D. *J. Colloid Interface Sci.* **1992**, *148*, 129–141.
(44) Khlebtsov, N. G. *Anal. Chem.* **2008**, *80*, 6620–6625.
(45) Kamat, P. V. *J. Phys. Chem. B* **2002**, *106*, 7729–7744.
(46) Wang, G.; Sun, W. *J. Phys. Chem. B* **2006**, *110*, 20901–20905.
(47) Wiederrecht, G. P.; Wurtz, G. A.; Bouhelier, A. *Chem. Phys. Lett.* **2008**, *461*, 171–179.
(48) Wiederrecht, G. P.; Wurtz, G. A.; Hranisavljevic, J. *Nano Lett.* **2004**, *4*, 2121–2125.

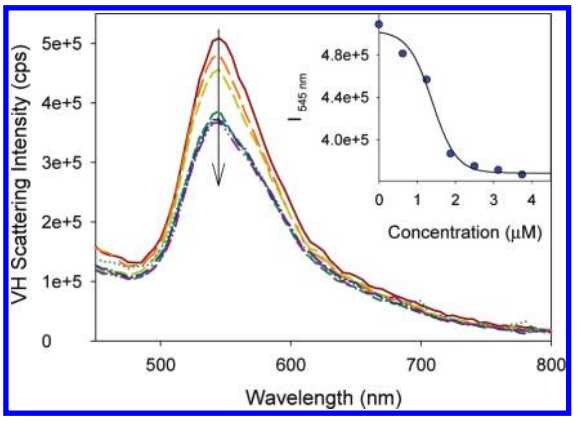


**Figure 3.** Depolarized light scattering spectra (parallel polarized source and perpendicularly polarized detection) from AuNPs after addition of specific amounts of PDE-1. Inset shows change in scattering intensity as a function of concentration of PDE-1 added, because no change in the shape of the particle is expected upon formation of the self-assembled monolayer on the AuNPs.

In this study we have followed a similar strategy by using a negatively charged phenyldithioester, PDE-1 (see Figure 2), to stabilize AuNPs, which has allowed us to study in detail the effect of adsorption of phenyldithioesters on the electronic properties of the AuNPs. PDE-1 is expected to bind to the AuNPs via the sulfur containing moiety and the carboxylate was expected to act as a charge stabilizing group. After addition of excess of PDE-1 to a solution of citrate stabilized AuNPs, no significant change was observed in the number average particle size or the *Z*-average (see Supporting Information for more detail). The fact that the no significant change was observed for the Z-average size in particular, which is more sensitive to larger particles in the distribution and hence any aggregates, demonstrates that no significant aggregation was occurring as a result PDE-1 addition. TEM images were also collected for as synthesized citrate stabilized AuNPs and AuNPs stabilized with PDE-1 (see Supporting Information). For both samples, it was generally observed that no aggregation was observed, but the occasional dimer or trimer was observed for both samples, which we attribute to drying artifacts that occur as a consequence of sample preparation. Importantly, the images demonstrate that there is no significant difference between the as-synthesized AuNPs and those that have been stabilized with PDE-1.

To further determine whether aggregation was occurring the samples were analyzed with depolarized light scattering. As well as an absorption component, Mie theory also predicts that AuNPs will also have a scattering component. Depolarized light scattering can sensitively assess the scattering component of the SPR.[49−52] Figure 3 shows the depolarized light scattering (vertically polarized source and horizontally polarized detection) from AuNPs after addition of specific amounts of PDE-1. The use of cross-polarization allows the Rayleigh scattering to be screened, so that depolarized scattering associated with the SPR can be highlighted. Addition of PDE-1 results in a small reduction of the scattering efficiency of the AuNPs. Drozdowicz-Tomsia et al.[50] have attributed the observation of depolarized scattering of AuNPs to be a result of their nonspherical geometry. Our particles also exhibit a geometry that is slightly nonspherical. The onset of aggregation of gold nanoparticles would be expected to result in, at the very least, the formation of a small number of nanoparticle dimers. Dimers formed from particles of the same size would result in elongated 'particles' which are analogous to a nanorod with a 2:1 aspect ratio. According to calculations by Khlebstov et al.[53] gold nanorods with an aspect ratio of 2 and a width of 15 nm would result in a scattering spectrum with a maximum at approximately 590 nm, as well as depolarized scattering intensity at the maxima that is enhanced by a factor of approximately 15, when compared to particles with an aspect ratio of approximately 1.2. This means that depolarized light scattering is very sensitive to the occurrence of even small degrees of aggregation. The depolarized light scattering spectra that are shown in Figure 3 do not exhibit any increase in the depolarized light scattering intensity with addition of PDE-1 to the solution of nanoparticles at wavelengths greater than 590 nm, which is consistent with no aggregation occurring in the system.

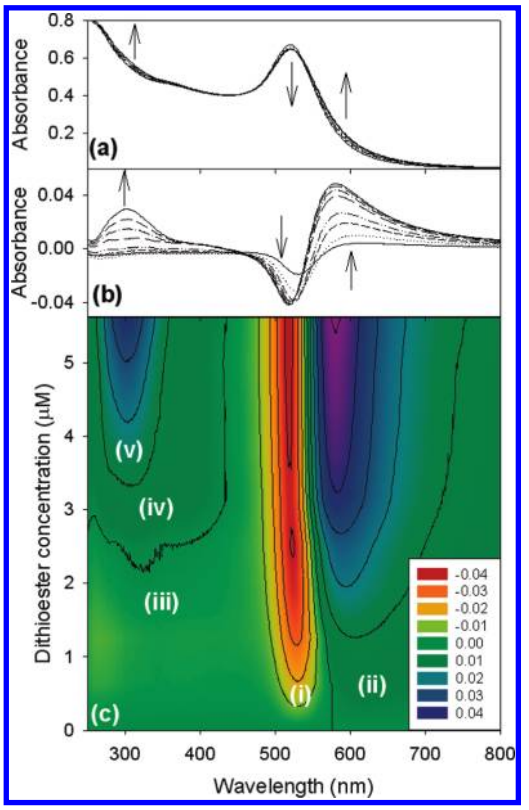


**Figure 4.** (a) UV−vis spectra showing the subtle changes in molecular the SPR upon addition of PDE-1 to a solution of AuNPs. (b) UV−vis difference spectra after addition of aliquots of PDE-1 to as synthesized AuNPs. (c) UV−vis contour map showing concentration dependent changes in SPR and molecular resonance upon addition of PDE-1 to AuNPs.

The UV−vis spectrum of a solution of PDE-1 in water exhibits an intense peak at 300 nm, which can be assigned to a strongly allowed $\pi-\pi^*$ transition of the phenyl group (see Figure 1). The UV−vis spectra after sequential addition of PDE-1 to AuNPs are shown in Figure 4a. The amounts added ranged from submonolayer coverage up to an excess of PDE-1. The UV−vis spectra are

(49) Calander, N.; Gryczynski, I.; Gryczynski, Z. *Chem. Phys. Lett*. **2007**, *434*, 326–330.
(50) Drozdowicz-Tomsia, K.; Xie, F.; Calander, N.; Gryczynski, I.; Gryczynski, K.; Goldys, E. M. *Chem. Phys. Lett*. **2009**, *468*, 69–74.
(51) Gryczynski, Z.; Lukomska, J.; Lakowicz, J. R.; Matveeva, E. G.; Gryczynski, I. *Chem. Phys. Lett*. **2006**, *421*, 189–192.
(52) Klitgaard, S.; Shtoyko, T.; Calander, N.; Gryczynski, I.; Matveeva, E. G.; Borejdo, J.; Neves-Petersen, M. T.; Petersen, S. B.; Gryczynski, Z. *Chem. Phys. Lett*. **2007**, *443*, 1–5.
(53) Khlebtsov, N. G.; Melnikov, A. G.; Bogatyrev, V. A.; Dykman, L. A.; Alekseeva, A. V.; Trachuk, L. A.; Khlebtsov, B. N. *J. Phys. Chem. B* **2005**, *109*, 13578–13584.

dominated by the SPR of the AuNPs, and changes after addition of PDE-1 are subtle. To amplify these changes, a spectrum of as-synthesized citrate stabilized AuNPs was subtracted from each of the other spectra (see Figure 4b). A contour plot of PDE-1 concentration versus wavelength is shown in Figure 4c. At concentrations of PDE-1 less than 3.5 $\mu$M the incremental changes observed are not simple additions of the spectra of the AuNP and PDE-1. After addition of amounts that correspond to a submonolayer of PDE-1, damping of the SPR maxima is observed (Figure 4c(i)), at the same time enhancement of the SPR band on the low frequency shoulder is also observed (Figure 4c(ii)). For a nonaggregating system there are two modes in which a small molecule can disrupt the SPR of AuNPs. The first is for a noninteracting molecule where the change in refractive index surrounding the particle causes a bathochromic shift of the entire SPR band. For example, this has been observed when AuNPs were transferred to different solvents.[45] However, we can not attribute the changes that occur during adsorption of PDE-1 to AuNPs to a mere change in the dielectric constant, because we are observing specific damping of the SPR at the maxima, enhancement in the low energy shoulder and no change in the high energy shoulder. Therefore, we attribute these changes to the formation of an AuNP$\cdots$PDE-1 charge transfer complex.

The $\pi-\pi^*$ band of PDE-1 at 300 nm is strongly bleached for solutions that contain 0.6−2.5 $\mu$M of PDE-1 (Figure 4c(iii)). At a PDE-1 concentration of 3.1 $\mu$M a broadened band that extends from 250 to 450 nm can be observed (Figure 4c(iv)). The bleaching of the $\pi-\pi$ * transition, which were observed to occur for solutions that contain below 3.4 $\mu$M of PDE-1, can also be attributed to a AuNP$\cdots$PDE-1 charge transfer complex. For solutions that contain above 3.8 $\mu$M of PDE-1 the undistorted $\pi-\pi^*$ band at 300 nm can be observed to increase linearly with concentration (Figure 4c(v)). This linear increase of the undistorted band can be attributed to absorbance by free PDE-1 in solution. Also of note is that an isosbestic point is observed at approximately 450 nm, which is consistent with a binding of PDE-1 occurring via complexation equilibrium.

The equilibrium process for the formation of a charge transfer complex between AuNPs and PDE-1 can be represented by the following equation:

$$\mathrm{Au}-* + \mathrm{PDE} \rightleftharpoons \mathrm{Au}-\mathrm{PDE} \qquad (1)$$

Where Au−* represents accessible free sites on the AuNPs and Au−PDE is the charge transfer complex. From the UV difference spectra, at high concentrations the amount of free PDE-1 ($[PDE]_{free}$) can be estimated by measuring the intensity of the $\pi-\pi^*$ transition at 300 nm. This then allows the amount of adsorbed PDE-1 to be calculated and hence the concentration of Au−PDE at saturation. Concentration curves for Au−PDE were calculated by measuring the absolute change in optical density of the SPR band between 450 and 900 nm where the concentration at saturation was used as a calibration point (Figure 5). The $[PDE]_{free}$ curve was calculated by subtracting [Au−PDE] from $[PDE]_0$ and the [Au−*] curve was calculated by subtracting $[PDE]_{free}$ from $[Au-*]_0$. A $[Au-*]_0$ of 5.28 $\mu$M, was estimated from the AuNP concentration (1.05 nM), AuNP surface area (804 $nm^2$) and the footprint of PDE-1 in a perpendicular orientation (0.16 $nm^2$). By plotting $[PDE]_{free}/[Au-PDE]$ versus $[PDE]_{free}$ (Figure 6), the concentration of the charge transfer complex at saturation, $\Gamma_{max}$, and the adsorption equilibrium constant, $K_{ads}$, can be calculated from the slope and intercept of

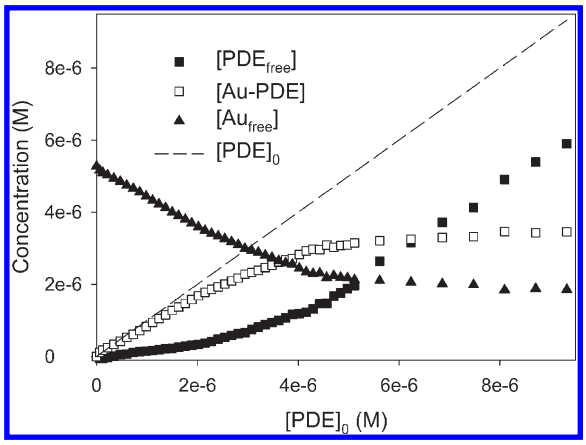


**Figure 5.** Plot shows change in concentration of free PDE-1 ($[PDE_{free}]$, filled squares), AuNP$\cdots$PDE-1 charge transfer complex ([Au−PDE], open squares) and unbound sites on the AuNP ([Au−*], filled triangles) as a function of the concentration of PDE-1 added ($[PDE]_0$, dotted line). The.

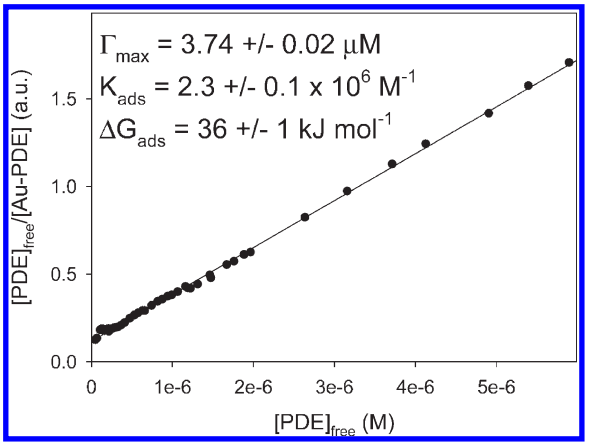


**Figure 6.** Plot of $[PDE]_{free}/[Au-PDE]$ versus $[PDE]_{free}$. Linear regression analysis results in a $\Gamma_{max}$ of 3.74 ± 0.02 $\mu$M and a $K_{ads}$ of 2.3 ± 0.1 × $10^6$ $M^{-1}$. The $K_{ads}$ corresponds to a $\Delta G$ of 36 ± 1 kJ $mol^{-1}$.

the graph. These were calculated to be 3.74 ± 0.02 $\mu$M and 2.3 ± 0.1 × $10^6$ $M^{-1}$ respectively. A $\Gamma_{max}$ of 3.74 ± 0.02 $\mu$M corresponds to a coverage of approximately 71%. Presumably greater coverage is prohibited by repulsion of the negatively charged molecules bound on the surface. From a $K_{ads}$ of 2.3 ± 0.1 × $10^6$ $M^{-1}$, the free energy of adsorption, $\Delta G$, can be calculated to be 36 ± 1 kJ $mol^{-1}$, which is comparable to that determined for the binding of thiols to gold surfaces[54] and to certain hydrogen bonding systems.[55] This is significant, because it demonstrates that PDE functionalized molecules can be used similarly to thiols for the functionalization of AuNPs.[56] For example, the phenyldithioester−AuNP interaction will be reversible, which means that exchange of phenyldithioesters should be able to be performed to tune the functionality of the AuNP surface. In the introduction we detailed that a structurally diverse range of phenyldithioesters and related compounds have been reported in the literature. The significance

(54) Jakubowicz, A.; Jia, H.; Wallace, R. M.; Gnade, B. E. *Langmuir* **2005**, *21*, 950–955.

(55) Binder, W.; Zirbs, R., Supramolecular Polymers and Networks with Hydrogen Bonds in the Main- and Side-Chain. In *Hydrogen Bonded Polymers*; Springer-Verlag: Berlin, Heidelberg, 2007; pp 1-78.

(56) Shaffer, A. W.; Worden, J. G.; Huo, Q. *Langmuir* **2004**, *20*, 8343–8351.

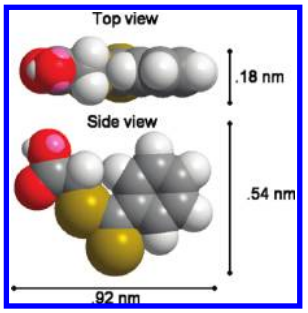


**Figure 7.** Space filling structures of energy minimized PDE-1.

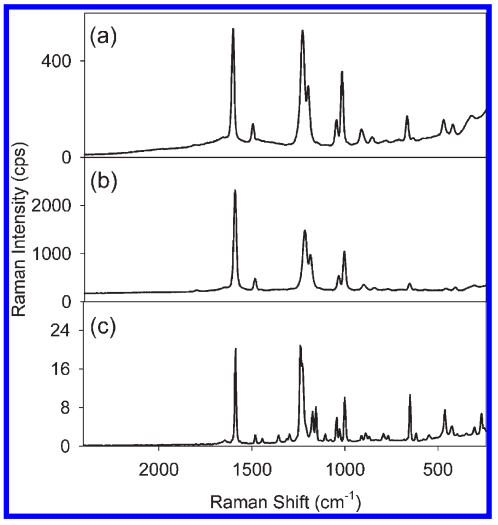


**Figure 8.** SERS of PDE-1 from an AuNP colloid solution with an excitation wavelength of, (a) 780 nm (32 scans) and (b) 633 nm (32 scans). (c) FT-Raman of PDE-1 with an excitation wavelength of 1064 nm (256 scans).

of strong interactions between phenyldithioesters and AuNPs reported here is that these molecules can be used for AuNP functionalization.

On the basis of the AuNP size determined by TEM and the amount of gold salt added during synthesis, the AuNP concentration for an as-synthesized solution of AuNPs that has been diluted by a factor of 2 can be estimated to be 1.05 nM. In the above analysis a $\Gamma_{max}$ of 3.74 ± 0.02 $\mu$M was determined from UV−vis spectroscopy. This corresponds to approximately 3560 molecules per NP. A number of methods are available to approximate the surface area of AuNPs. In this case we have approximated the AuNPs as spheres. This results in a calculated surface area of 804 nm$^2$ for AuNPs with a diameter of 16 nm, which corresponds to a minimum footprint of 0.22 nm$^2$ per molecule. In the unbound form MM2 energy minimization of the structure of PDE-1 results in a planar molecule, the theoretical footprints for perpendicular and flat binding conformations are 0.16 and 0.50 nm$^2$ respectively (see Figure 7). It should be noted that these values do not take into account any distortions of the molecule that may occur due to attachment to the surface, or repulsive forces that occur as a result of the negatively charged molecules. The footprint estimated from the UV titration is intermediate between the flat and perpendicular footprints, which indicates that the molecule can not be in a flat binding conformation. However, due to the uncertainty regarding the exact surface conformation of the molecule it is not possible to comment with certainty on the precise angle of the molecule to the surface.

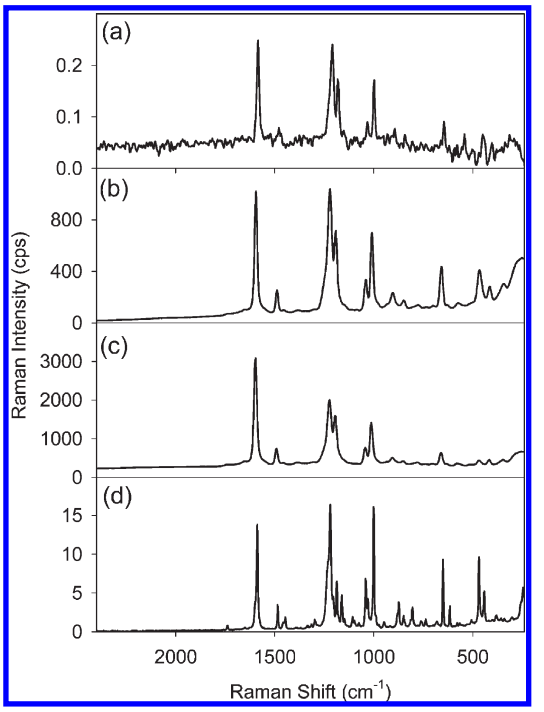


**Figure 9.** SERS of PDE-2 from an AuNP colloid solution with an excitation wavelength of (a) 1064 nm (4096 scans), (b) 780 nm (32 scans), and (c) 633 nm (32 scans). (d) FT-Raman of PDE-2 with an excitation wavelength of 1064 nm (256 scans).

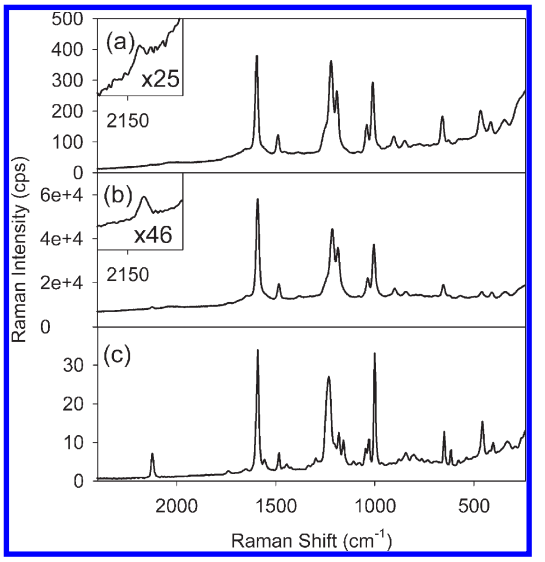


**Figure 10.** SERS of PDE-3 from an AuNP colloid solution with an excitation wavelength of (a) 780 nm (32 scans) and (b) 633 nm (32 scans). (c) FT-Raman of PDE-3 with an excitation wavelength of 1064 nm (256 scans). Insets for parts a and b show C≡C str, where the number corresponds to the magnifying multiplier.

## SERS of Phenyldithioester−AuNP Complexes and FT Raman of Phenyldithioesters

Solutions of AuNPs stabilized with PDE-1 did not yield significant SERS spectra. This is not unexpected because the theoretical enhancement factor expected from single AuNPs is in the vicinity of only 30−40 times,[57] and experimentally SERS is

(57) Franzen, S. *J. Phys. Chem. C* **2009**, *113*, 5912–5919.
(58) Laurence, T. A.; Braun, G.; Talley, C.; Schwartzberg, A.; Moskovits, M.; Reich, N.; Huser, T. *J. Am. Chem. Soc.* **2009**, *131*, 162–169.

**Table 1. Peak Assignments for FT-Raman and SERS of PDE-1, -2, and -3**

| FT-Raman PDE-1 | SERS PDE-1 | FT-Raman PDE-2 | SERS PDE-2 | FT-Raman PDE-3 | SERS PDE-3 | mode |
|---|---|---|---|---|---|---|
| | | | | 2122 | 2120 | C≡C str |
| | | 1737 | | 1739 | | C═O str |
| 1588 | 1587 | 1588 | 1588 | 1590 | 1587 | quadrant $\nu_{2\text{-CC}}$, in-plane[b] |
| 1481 | 1480 | 1485 | 1480 | 1484 | 1480 | semicircle $\nu_{3\text{-CC}}$, in-plane[b] |
| 1443 | | 1446 | | 1444 | | $\nu_{4\text{-CC}}$, in-plane[b] |
| 1297 | | 1297 | | 1297 | | $\beta_{CH}$, in-plane |
| 1232 | 1212 | 1219 | 1212 | 1232 | 1210 | C═S str |
| 1174 | 1183 | 1186 | 1184 | 1181 | 1182 | $\beta_{CH}$, in-plane[b] |
| 1161 | | 1154 | | 1158 | | $\beta_{CH}$[b] |
| 1105 | | 1106 | | 1107 | | $\nu_{CS}$? |
| 1076 | | 1074 | | 1077 | | $\beta_{CH}$[b] |
| 1044 | | 1041 | | 1045 | | $\nu_{CS}$? |
| 1027 | 1030 | 1029 | 1030 | 1029 | 1031 | $\beta_{CH}$[b] |
| 1000 | 1000 | 1000 | 1000 | 1000 | 1000 | "ring breathing" $\beta_{CCC}$[b] |
| | | 990 (sh) | | | | out of plane[b] |
| | | 972 | | 965 | | $\gamma_{CH}$ out of plane |
| 888 | 895 | 873 | 895 | 878 | 895 | $CH_2$ in ester[a] |
| 868 | 838 | 849 | 839 | 843 | 839 | $\gamma_{CH}$ out of plane |
| 792 | | 804 | | 802 | | in plane |
| 767 | | 767 | | 732 | | $\gamma_{CH}$ |
| 649 | 649 | 650 | 650 | 649 | 650 | C−S |
| 616 | | 615 | 618 | 616 | | $\beta_{CCC} + \nu_{CS}$? |
| 462 | 454 | 468 | | 457 | 464 | in-plane |
| | | 442 | 455 | | | associated with ester[a] |
| 424 | 403 | 400 | 402 | 402 | 414 | out of plane |
| 345 | | 309 | | | 343 | $\beta_{CS}$ |

[a] From comparison with spectra from α methyl bromophenylacetate, α-ethyl-bromophenylaceate, and α-ethyl-chlorophenylaceate (see Supporting Information for spectra). [b] Based on assignments from benzyl thiol (Szafranski et al.[61]).

typically not observed or is very weak for small single AuNPs.[58−60] After addition of a small amount of brine the color of the solution changed from red to purple was observed and particle aggregation was observed by TEM (see Supporting Information) For this aggregated sample an intense SERS spectrum was observed (Figure 8a) for excitation at 633 and 780 nm. For comparison the FT-Raman of PDE-1 is shown in Figure 8b. Addition of PDE-2 and -3 where the concentrations were above the critical aggregation concentration also resulted in a change in the gold colloid solution from red to purple and aggregation was also observed by TEM (see Supporting Information). Again for these aggregated particles an intense SERS spectra (see Figure 9 and Figure 10, respectively) for excitation wavelengths of 633 and 780 nm. A weak SERS spectrum was observed using an excitation wavelength of 1064 nm for PDE-2 (see Figure 9 a) (Similar spectra were observed for PDE-1 and -3, but the data are not shown). For comparison the FT Raman of PDE-2 and -3 are shown in Figure 9d and Figure 10c, respectively. The Raman or SERS spectra of the PDE-1, -2, and -3 or their assignments have not been previously reported.

**Assignment of Major Common Peaks in FT Raman Spectra.** The assignments for the normal Raman of the phenyldithioesters are shown in Table 1. These assignments have been based on previous reports of the assignment of Raman spectra of benzyl thiol (BT) and dibenzyl disulfide (DBDS),[61] general literature Raman assignments for relevant functional groups,[62] as well as comparison of the Raman spectrum of PDE-2 and -3 with the Raman spectrum of α-bromophenylacetate (BPA) (see Supporting Information). Only the major vibrational modes and those important for the discussion of the SERS spectra are discussed below.

The band at 1000 $cm^{-1}$ can be assigned to in-plane ring breathing of the aromatic ring. For monosubstituted benzene compounds, such as toluene and BPA this band is typically the strongest Raman scatterer and its Raman shift and intensity are substituent independent, so it will be used as an internal standard to compare the relative intensities of other band in the spectrum. PDE-2 and -3 have two monosubstituted phenyl groups in their structures and as such have ring breathing peaks in the normal Raman spectrum that are approximately twice as strong as for PDE-1, which has only one monosubstituted phenyl group in the structure. The band at 1588 $cm^{-1}$ can be assigned to the aromatic quadrant CC stretch, for monosubstituted benzenes. The peak intensity is very strong when compared to the spectrum of toluene (see Supporting Information). For example, the ratio of the bands at 1588 and1000 $cm^{-1}$ is sixty times greater for PDE-4 than it is for toluene. A possible reason for this is the conjugation of the C═S bond to one of the aromatic rings. A similar increase in intensity is observed for other monosubstituted benzenes with substituents that are conjugated with the aromatic ring, such as butyl benzoate and styrene (See Supporting Information). The band at 1486 $cm^{-1}$ can be assigned to the semicircle CC stretch for monosubstituted benzenes,[61,62] The band at 1186 $cm^{-1}$ can be assigned to an aromatic C−H in-plane bend. The band at 1030 $cm^{-1}$ can be assigned to semicircle stretch mixed with the in-plane bend.[61]

**Assignment of Modes Associated with the Dithioester.** Assignment of peaks associated with C═S and C−S is complicated because it is known that these vibrational modes have a tendency to couple with adjacent vibrational modes.[62] As a result of this C═S stretching bands have been reported over a wide range of frequencies.[62] There have been a number of reports on the assignment of bands associated with aliphatic dithioester

(59) Alvarez-Puebla, R. A.; Arceo, E.; Goulet, P. J. G.; Garrido, J. J.; Aroca, R. F. *J. Phys. Chem. B* **2005**, *109*, 3787–3792.
(60) Brown, L. O.; Doorn, S. K. *Langmuir* **2008**, *24*, 2178–2185.
(61) Szafranski, C. A.; Tanner, W.; Laibinis, P. E.; Garrell, R. L. *Langmuir* **1998**, *14*, 3570–3579.
(62) Lin-Vien, D.; Colthup, N. B.; Fateley, W. G.; Grasselli, J. G., *The Handbook of Infrared and Raman Characteristic Frequencies of Organic Molecules*; Academic Press: San Diego, CA, 1991.

vibrational modes,[63−66] where bands at 1192 $cm^{-1}$ were assigned to the C═S stretching mode. There has only been a single report of the Raman assignment of aromatic dithioesters, which was a chloro-substituted aromatic dithioester and a peak at 1237 $cm^{-1}$ was assigned to the C═S stretch.[67] Diarylthioketones have been reported to have C═S stretching modes in the 1205−1225 $cm^{-1}$.[68] Based on these literature assignments, comparison with Raman spectra small molecule analogues such as toluene and α-bromophenylacetate (see Supporting Information) the C═S stretch of the dithioester group for PDE-1, -2, and -3 can be assigned peaks at 1238, 1219, and 1230 $cm^{-1}$, respectively. The different Raman shifts for the C═S band for these compounds suggests that, like the C═O stretching mode, the C═S stretching mode is sensitive to its environment, e.g. the dielectric constant of the immediate vicinity and hydrogen bonding.[69] The intensity of the C═S stretch for PDE-1, -2, and -3 is very strong. Aliphatic dithioesters have been reported to have a medium intensity C═S band relative to the 1000 $cm^{-1}$ ring breathing mode.[70] The intensity of the C═S band for 4-chlorophenyldithioester, reported by Dong et al.[67] was one of the strongest bands in the spectrum, but due to the para-substitution of the aromatic ring no ring breathing mode was available for comparison of band intensities. Conjugation of the thiocarbonyl with the aromatic ring would be expected to result in enhanced intensity of the C═S vibrational mode, due to an increase in polarizability. Similar enhancements are observed for the C═O stretch of benzoates (see Supporting Information). The strong intensity of C═S bands for PDE-1, −2, and −3 is also consistent with assignment of this band as a C═S stretch.

The frequency of the C−S stretching mode has been reported to be sensitive to substituents.[63] However, based on literature reports of the C−S stretch and comparison with the Raman spectrum of α-bromophenylacetate, the band at 651 $cm^{-1}$ can be assigned to the C−S stretching mode. Other bands at 1041, 468, and 442 $cm^{-1}$ are also believed to be associated with vibrational modes of the dithioester. A tentative assignment of the 468 and 442 $cm^{-1}$ bands are S═C−S and C−C═S bending modes respectively.[66]

## Analysis of the SERS Spectra

**Description of SERS Results.** As seen in Table 1 the dominant bands observed in the 780 nm SERS spectra can be divided into two groups: (1) those associated with in-plane vibrational modes (1588, 1480, 1183, 1030, and 1000 $cm^{-1}$); (2) those associated with substituents $CH_2$ 896 ($cm^{-1}$), C═S (1212 $cm^{-1}$), C−S stretch (650 $cm^{-1}$) and other bands associated with the dithioester group (468 and 442 $cm^{-1}$). A weak band is also observed at 839 $cm^{-1}$ which may be associated with an out-of-plane mode, but assignments in this region of the spectrum are relatively uncertain. For PDE-1 each of these groups has been enhanced to approximately the same degree as those observed in the in the normal Raman spectrum. For PDE-2 and -3, the degree of enhancement only differs for the ring breathing band at 1000 $cm^{-1}$, where the intensity has approximately halved compared to the other peaks.

**Mode of Binding.** A key result from these SERS experiments is that the C═S stretching band exhibits a significant shift compared to the normal Raman, while the C−S band and bands associated with the aromatic ring exhibit no significant shift. The C═S band shift ranged from 6 to 25 $cm^{-1}$ depending of the structure of the phenyl dithioester. From this it can be concluded that the mode of binding for the small molecule phenyl dithioesters is monodentate through the C═S sulfur, and there is no significant interaction of the phenyl ring, or the C−S sulfur, with the gold nanoparticle surface. It is also interesting to note that in each case the shift observed for the C═S stretch as a result of binding was to approximately 1210−1212 $cm^{-1}$, regardless of the frequency of the band in the normal Raman spectrum. This indicates that the nature of the C═S vibrational modes of the C═S sulfur bound to gold are strongly influenced by the gold−sulfur interactions. The fact that the C═S and C−S stretches are still observed indicates that the dithioester does not disassociate upon binding. Further support of this is that for PDE-3 the C≡C stretch of the terminal acetylene can be seen in the SERS, although substantially less intense relative to the major peaks (see Figure 10). The reason for the change in relative intensities will be discussed later in the text.

The above data indicates that the binding of phenyldithioesters to AuNPs is monodentate through the C═S sulfur. This is in contrast to the results reported by Duwez et al.,[21] who used X-ray photoelectron spectroscopy (XPS) to demonstrate that the particular phenyldithioester they were studying was binding in a bidentate fashion. There are a number of reasons for the differences in the results obtained from XPS and SERS. The first is surface coverage of the phenyldithioester. Duwez and co-workers experiments were carried out on flat gold surfaces. Although they did not specifically measure the surface coverage of the phenyldithioester small molecules used in their study, the experimental conditions and choice of a non charged phenyldithioester for self-assembled monolayer formation would be consistent with a high degree of surface coverage. In contrast, the maximum coverage of PDE-1, a negatively charged molecule, was 71%. It was not possible to measure the coverage of the PDE-2 and -3, but the mode of preparation is not likely to result in a high coverage of molecules in the nanogap between two AuNPs. The degree of coverage has been shown to affect the mode of binding of thiols[71] and dithiocarbamates;[13] hence, it is likely to have an effect for the binding of phenyldithioesters to AuNPs as well.

Other factors that may explain the differing results, is that the SERS experiments have been carried out in solution, while the XPS has been carried out at high vacuum, and the incident X-rays or photoelectrons formed during analysis may result in X-ray induced degradation of the phenyldithioester molecules in the self-assembled monolayers. X-ray degradation of the phenyldithioester molecule would be likely to result in a different binding mode. This makes interpretation of the spectra difficult, in addition to the fact that the XPS spectra have been taken close to the limit of detection for sulfur.

**Explanation of Enhancement.** There are three resonance conditions that have been demonstrated to affect the enhancement observed in SERS. The first is surface plasmon resonance, where the polarizability tensors of a metal-molecule adduct couple to the SPR field. For gold, only limited enhancement is expected from single, unaggregated particles.[57−60] A number of

(63) Ozaki, Y.; Storer, A. C.; Carey, P. R. *Can. J. Chem.* **1982**, *60*, 190–198.
(64) Storer, A. C.; Ozaki, Y.; Carey, P. R. *Can. J. Chem.* **1982**, *60*, 199–209.
(65) Teixeira-Dias, J. J. C.; Jardim-Barreto, V. M.; Ozaki, Y.; Storer, A. C.; Carey, P. R. *Can. J. Chem.* **1982**, *60*, 174–189.
(66) Fausto, R.; Martins, A. G.; Teixeira-Dias, J. J. C.; Tonge, P. J.; Carey, P. R. *J. Phys. Chem.* **1994**, *98*, 3592–600.
(67) Dong, J.; Luo, L.; Liang, P.-H.; Dunaway-Mariano, D.; Carey, P. R. *J. Raman Spectrosc.* **2000**, *31*, 365–371.
(68) Socrates, G. *Infrared and Raman Characteristic Group Frequencies*; 3rd ed.; John Wiley & Sons: Chichester, U.K., 2004.
(69) Bellamy, L. J.; Rogasch, P. E. *J. Chem. Soc.* **1960**, 2218–2221.
(70) Varughese, K. A.; Angus, R. H.; Carey, P. R.; Lee, H.; Storer, A. C. *Can. J. Chem.* **1986**, *64*, 1668–1673.
(71) Rodriguez, J. A.; Dvorak, J.; Jirsak, T.; Liu, G.; Hrbek, J.; Aray, Y.; Gonzalez, C. *J. Am. Chem. Soc.* **2003**, *125*, 276–285.

groups have shown that significant enhancements in electric field occur in the nanogap between nanoparticle dimers or aggregates.[72−74] The second resonance is via charge transfer resonance, which involves transfer of electrons between the conduction band of a metal and a small molecule complexed with, or weakly bound to the metal.[75−77] The third and final resonance is molecular resonance. Lombardi and Birke.[78,79] have presented a unified expression to describe the SERS phenomena, where these three types of resonance are combined. For a full description of this expression and its consequences for interpretation of SERS the reader is directed to reviews and articles by Lomardi and Birke.[78,79] Briefly, their theory shows how the three resonance conditions can be thought to be interrelated. Due to the fact that these terms are products of each other a number of groups have demonstrated that the interpretation of SERS spectra needs to take all these aspects into consideration.[77,79−81] For example, as will be shown below, even when the excitation frequency is far from a charge transfer resonance, it can still have a large influence on the spectra.

For the systems studied in this work, there is little overlap of the excitation wavelength at 785 and 1064 nm with the AuNP···PDE-1 charge transfer-resonance. In this situation Lombardi and Birke's unified expression for SERS predicts that SPR effects will dominate the spectrum, and hence only totally symmetric modes will be strongly enhanced, which is what was observed, apart from the ring breathing mode at 1000 $cm^{-1}$ for PDE-2 and -3. This can be explained by the fact that the three resonance terms in the theory are inextricably linked so that even far from a charge transfer resonance, charge transfer can still strongly affect the appearance of a spectrum. In this case, the ring breathing mode from the pendant phenyl group does not appear in the SERS spectrum. This is a result of the phenyldithioester dominating the charge transfer complex, because this group is conjugated to the AuNP surface via the C═S bond. In contrast, the pendant phenyl group is not conjugated to the AuNP, and hence, its contribution to the charge transfer complex will be small. The same argument can be applied to explain the small enhancement observed for the C≡C stretch at 2122 $cm^{-1}$ for PDE-3; i.e., the acetylene group is not conjugated to the AuNP surface and so does not participate significantly in the charge transfer complex with the AuNP. Hence, this vibrational mode only exhibits a much smaller degree of enhancement.

Calculations made by Shegai et al.[73] have shown that the electric field in between nanoparticle dimers is aligned perpendicular to the nanoparticle surfaces and the greatest electric field enhancements occur when a dipole is aligned parallel to the electric field or normal to the particle surfaces. These enhancements are 5 orders of magnitude greater when compared to dipoles that are perpendicular to the electric field. However, it should be noted that most of this enhancement (approximately 3 orders of magnitude) occurs from perpendicular to about 15° off perpendicular to the electric field and there is relatively little difference between 45° off-perpendicular and parallel to the electric field. PDE-1 is planar and thus has $C_s$ symmetry. Results described above show that the binding of the molecule takes place through a C═S···Au interaction. From this mode of binding, we would expect the aromatic ring to be oriented close to perpendicular to the AuNP surface or parallel to the electric field. This is consistent with the UV-titration results described above. The charge transfer transition moment is also expected to be parallel to the molecular plane and hence approximately perpendicular to the Au surface. There are a number of low lying excited states, which are available for intensity borrowing. These are the weak $n-\pi^*$ transition at 475 nm (2.61 eV), the moderate $\pi-\pi^*$ transition at 300 nm (4.14 eV), and a strong transition at ∼190 nm (6.53 eV). The charge transfer transition for the AuNP phenyldithioester complex occurs at approximately 580 nm (2.14 eV). Hence, it is conceivable that when using an excitation wavelength of 633 nm (1.96 eV) vibronic coupling of the ground state of the molecule with the metal−molecule CT state occurs, and is dictated by the Herzberg−Teller coupling constant. This then allows excitation of the molecular excited state from the metal−molecule CT state. Hence, it can be predicted that the in-plane modes should be selectively enhanced, which is what we have observed. The enhancement of the C═S band at 1214 $cm^{-1}$ and to a lesser extent the C−S band at 650 $cm^{-1}$ can be attributed to the conjugation that occurs between this substituent and the phenyl group. The consequence of this conjugation is that the phenyldithioester group must be considered as an extended $\pi$ system and it would be expected that the C═S and to a lesser extent the C−S bonds will be vibrating in the plane of the aromatic ring. These findings reiterate those observed by other groups for molecules such as pyridine and other azine type compounds.[79]

Phenyldithioester derivatives which exhibit intense SERS spectra will impact on the field of spectroscopically barcoded NPs or NP aggregates. Phenyldithioester type molecules will be able to be used as molecular barcodes for these sorts of assemblies. The results shown in this study indicate that the phenyl group adjacent to the C═S dominates the SERS spectra with relatively little contribution from groups pendant to the phenyldithioester. Hence, development of further dithioester based molecular barcodes should focus on modifying the phenyl group conjugated to the C═S. Another important implication of charge transfer complexes for SERS based molecular barcodes is that the choice of excitation wavelength needs to be considered. For example, if the phenyldithioesters in this study were to be used as molecular barcodes, it is important to know that the 633 nm and the 780 nm excitation wavelengths will result in different spectroscopic fingerprints.

## Conclusions

A study of the electronic and scattering spectra of solutions of phenyldithioesters and AuNPs shows that phenyldithioesters form a charge transfer complex with AuNPs, where a binding constant of $(2.3 \pm 0.1) \times 10^6\ M^{-1}$ and a Gibbs free energy of 36 ± 1 kJ $mol^{-1}$. This is of the same order as binding of thiols to gold and certain hydrogen bonding systems. From the number of bound molecules per AuNP it was determined that the orientation of the molecule was approximately perpendicular to the AuNP surface. Aggregation of the AuNPs was required to observe a SERS spectrum of the phenyldithioesters. The band assigned to C═S was the only band that was observed to have a significant shift compared to the normal Raman spectrum, which indicated that the mode of binding was monodentate via the C═S group for

(72) Talley, C. E.; Jackson, J. B.; Oubre, C.; Grady, N. K.; Hollars, C. W.; Lane, S. M.; Huser, T. R.; Nordlander, P.; Halas, N. J. *Nano Lett.* **2005**, *5*, 1569–1574.
(73) Shegai, T.; Li, Z.; Dadosh, T.; Zhang, Z.; Xu, H.; Haran, G. *Proc. Natl. Acad. Sci. U.S.A.* **2008**, *105*, 16448–16453.
(74) Michaels, A. M.; Jiang; Brus, L. *J. Phys. Chem. B* **2000**, *104*, 11965–11971.
(75) Lombardi, J. R.; Birke, R. L.; Lu, T.; Xu, J. *J. Chem. Phys.* **1986**, *84*, 4174–4180.
(76) Sun, Z.; Wang, C.; Yang, J.; Zhao, B.; Lombardi, J. R. *J. Phys. Chem. C* **2008**, *112*, 6093–6098.
(77) Canamares, M. V.; Chenal, C.; Birke, R. L.; Lombardi, J. R. *J. Phys. Chem. C* **2008**, *112*, 20295–20300.
(78) Lombardi, J. R.; Birke, R. L. *Acc. Chem. Res.* **2009**, *42*, 734–742.
(79) Lombardi, J. R.; Birke, R. L. *J. Phys. Chem. C* **2008**, *112*, 5605–5617.
(80) Kudelski, A.; Bukowska, J. *Chem. Phys. Lett.* **1996**, *253*, 246–250.
(81) Osawa, M.; Matsuda, N.; Yoshii, K.; Uchida, I. *J. Phys. Chem.* **1994**, *98*, 12702–12707.

these molecules. The formation of the charge transfer complex was found to significantly influence the appearance of the SERS spectra. At the charge transfer resonance it was found that the in-plane bands associated with molecular excited state were preferentially enhanced, which indicated that intensity borrowing was occurring via vibronic coupling of the molecular ground state and the charge transfer state. Away from the charge transfer resonance the symmetric bands associated with the charge transfer complex were enhanced preferentially over other symmetric bands in the molecules. The results from this study can impact on the development of functionalized nanoparticles and the choice of SERS tags and excitation wavelengths for use in spectroscopically barcoded NP assemblies.

**Acknowledgment.** This research was supported under the Australian Research Council's Discovery Projects and Linkage Equipment, Infrastructure, and Facilities funding schemes (project numbers DP0878615, DP0555879, LE0668517, and LE0775684). This work was performed in part at the Queensland node of the Australian National Fabrication Facility. A company established under the National Collaborative Research Infrastructure Strategy to provide nano- and microfabrication facilities for Australia's researchers. This work was performed in part at the Bio-Nano Development Facility, which was funded by the Queensland State Government Smart State Innovation Building Fund. Part of this work was performed while Dr Blakey was the recipient of a Queensland State Government Smart State Fellowship.

**Supporting Information Available:** Text giving a description of general characterization procedures and figures showing representative TEMs, and a figure aiding Raman peak assignments. This material is available free of charge via the Internet at http://pubs.acs.org.